# OBSERVATIONS ON THE MARGINAL BAND SYSTEM OF NUCLEATED ERYTHROCYTES

WILLIAM D. COHEN

From the Department of Biological Sciences, Hunter College of the City University of New York, New York 10021 and the Marine Biological Laboratory, Woods Hole, Massachusetts 02543

ABSTRACT

The marginal band (MB) of nucleated erythrocytes (those of nonmammalian vertebrates) is a continuous peripheral bundle of microtubules normally obscured by hemoglobin. Treatment of these elliptical cells with modified microtubule polymerization media containing Triton X-100 yields a semilysed system in which MB, nucleus, and trans-MB material (TBM) are visible under phase contrast. The TBM apparently interconnects structural components, passing around opposite sides of the nucleus and suspending it in native position. In uranyl acetate-stained whole mounts (goldfish) examined by transmission electron microscopy, the TBM appears as a network.

MBs of semilysed cells are relatively planar initially, but twist subsequently into a range of "figure-8" shapes with one of the two possible mirror-image configurations predominant. Nuclei and MBs can be released using proteolytic enzymes, to which the TBM seems most rapidly vulnerable. MBs thus freed are birefringent, generally untwisted, and much more circular than they are *in situ*. As a working hypothesis, it is proposed that the flattened, elliptical shape of nucleated erythrocytes is a result of TBM tension applied asymmetrically across an otherwise more circular MB, and that the figure-8 configuration occurs when there is extreme TBM shrinkage or contraction.

KEY WORDS marginal band · microtubules · nucleated erythrocytes · cellular morphogenesis

The marginal band (MB) in nucleated erythrocytes of nonmammalian vertebrates is a prominent microtubule system found just beneath the plasma membrane (20, 21). It is generally assumed to be involved in formation and/or maintenance of the flattened elliptical shape of such cells (21, 33), but its role is not well understood and has been brought into question by several investigators in recent years (4, 6, 8). Although fixation and staining can render the MB visible *in situ* for light microscopy (21, 33), hemoglobin obscures it in the living cell, constituting a major obstacle to experimentation. The purpose of this paper is to show that the MB can be visualized directly by light microscopy under certain semilytic conditions which permit hemoglobin escape while retaining major structural elements of the erythrocyte. Observations on the morphology of the system thereby obtained suggest a possible mechanism by which the MB functions in cell shape determination.

## MATERIALS AND METHODS

The following species were utilized in this work (1, 17):

*Amphiuma tridactylum* (giant salamander, or "Congo eel"), *Notophthalmus viridescens* (Eastern red-spotted salamander, or "newt"), *Cynops pyrroghaster* (Far-Eastern red-bellied salamander), *Rana pipiens* (leopard frog), *Rana catesbiana* (bullfrog), *Carassius auratus* (goldfish). Goldfish, salamanders, and a few specimens of *R. pipiens* were maintained in tanks at room temperature (21°–23°C) on diets of dry goldfish food, goldfish (for *Amphiuma*), tubifex worms (for other salamanders), and horseflies or ground beef (for frogs). *R. catesbiana* and most *R. pipiens* specimens were cold-stored in refrigerators at approx. 5°C for periods of up to 2 wk. Blood samples were obtained from salamanders by snipping the tail tip, from frogs by decapitation with pithing or by foot puncture, and from goldfish by decapitation or gill puncture. Whole blood was used immediately without additions (no anticoagulants), except for a few experiments in which frog cells were first washed free of serum by centrifugation or settling in amphibian Ringer's solution (Winton-Bayliss formula; reference 15).

The lytic medium (LyM) was based upon the in vitro microtubule polymerization conditions discovered by Weisenberg (46) as modified by Rebhun et al. (35) for mitotic apparatus preparation. It consisted of 100 mM piperazine-*N*-*N*′-bis[2-ethane sulfonic acid] (PIPES), 1 mM $MgCl_2$, 5 mM ethyleneglycol-bis-[$\beta$-aminoethyl ether]*N*,*N*′-tetraacetic acid (EGTA), 10 mM *p*-tosyl arginine methyl ester HCl (TAME), and 0.4% (wt/vol) Triton X-100, brought to pH 6.8 with KOH, with modifications in specific experiments. In this medium TAME is included as a precaution against proteolysis (35), while EGTA serves to reduce the $Ca^{++}$ below polymerization-inhibiting levels (46). Similar media have been used by others to stabilize microtubule-containing structures in semilysed mitotic cells (14, 29, 32).

Most of the light microscope observations were made with a Zeiss phase-contrast microscope equipped with Planachromat (16 ×, 25 ×) and Neofluar (40 ×, 100 ×) objectives (Carl Zeiss, Inc., New York). The darkfield effect was achieved with this microscope under ordinary illumination by employing the 16 × phase objective in conjunction with the 100 × condenser annulus. In some experiments a Zeiss polarizing microscope was also utilized. Microsurgery was performed on slides under phase contrast or darkfield in open Vaseline-bounded wells, with a Leitz micromanipulator (E. Leitz, Inc., Rockleigh, N. J.). Images were recorded on Kodak 35 mm Plus-X or Tris-X film.

Slides and cover slips were routinely soaked in Micro cleaning solution (International Products Corp., Trenton, N. J.) as a precaution against oily manufacturing films often contaminating them, with subsequent washing and drying. Vaseline was used for sealing cover slips to avoid drying or flattening of material during long-term observation; comparison of samples with and without Vaseline present showed that it had no effect on the material. Pieces of lens paper at open cover slip edges were used to control flow of media during perfusion experiments.

PIPES, EGTA, TAME, pepsin (P7012; from hog stomach mucosa, 1:60,000), and trypsin (T0134; from hog pancreas, type IX) were obtained from the Sigma Chemical Co. (St. Louis, Mo.); Triton X-100 from Sigma and Calbiochem (San Diego, Calif.). Media used in experiments were either freshly prepared or stored frozen stocks, as it was observed that bacteria had a propensity for growth in LyM and some of its components under refrigeration at 5°C.

For whole-mount staining of semilysed cells or free MBs for transmission electron microscopy (TEM), 1 ml preparations (1:10, blood:LyM) were centrifuged for 2 min at approx. 1,700 *g* in an International Clinical Centrifuge at room temperature. Sedimented material was washed by resuspension and similar centrifugation in 1–2 ml of LyM, and resuspended in 1 ml of LyM lacking Triton and TAME (= "wash medium") to which 1 ml of 5% gutaraldehyde in wash medium was subsequently added. After fixation at room temperature for 60 min, preparations were washed by a cycle of centrifugation, resuspension in 1–2 ml of wash medium, and recentrifugation as described previously. Sedimented material was resuspended to 0.2–0.5 ml in wash medium, and samples were placed on Formvar-coated grids for 2 min. Fluid was drawn off with filter paper, replaced by 2% aqueous uranyl acetate, drawn off again after 30 s, and the grids air-dried. Observations were made with the Hitachi HS-8 transmission electron microscope operating at 50 kV.

## EXPERIMENTS AND RESULTS

### *Initial Observations*

When fresh frog blood (*R. pipiens*) is diluted 1:10–1:100 into LyM at room temperature, the erythrocytes (Fig. 1*a*) hemolyze immediately. As seen in phase contrast, the partially lysed cells consist of nucleus and MB, with nearly invisible material keeping them together (Fig. 1*b*). The MB generally assumes a figure-8 configuration with the nucleus at the cross-over point, retaining the central position characteristic of the living cells (Fig. 1). The MB is approx. 0.3 $\mu$m thick and 25 $\mu$m from top to bottom of the figure-8, about the same length as the living frog erythrocyte (long axis of ellipse). The MB is easily seen in phase contrast, and careful focusing in different planes reveals its continuity and thickness uniformity. Tapping and pressing on the cover slip demonstrates that the nucleus is highly resistant to displacement and that the MB does not break easily.

### *Other Species*

Erythrocytes of *Amphiuma* were of interest because they are the largest known among the vertebrates (1), and have a relatively thick MB easily visible in the light microscope in stained

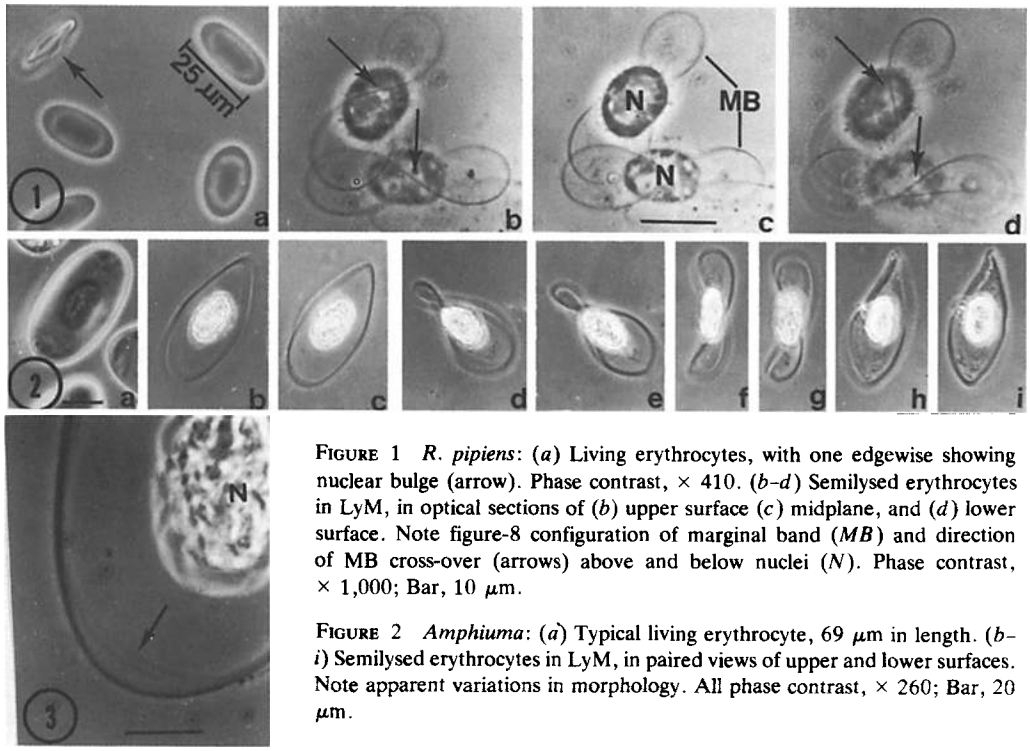


FIGURE 1 *R. pipiens*: (*a*) Living erythrocytes, with one edgewise showing nuclear bulge (arrow). Phase contrast, × 410. (*b–d*) Semilysed erythrocytes in LyM, in optical sections of (*b*) upper surface (*c*) midplane, and (*d*) lower surface. Note figure-8 configuration of marginal band (*MB*) and direction of MB cross-over (arrows) above and below nuclei (*N*). Phase contrast, × 1,000; Bar, 10 μm.

FIGURE 2 *Amphiuma*: (*a*) Typical living erythrocyte, 69 μm in length. (*b–i*) Semilysed erythrocytes in LyM, in paired views of upper and lower surfaces. Note apparent variations in morphology. All phase contrast, × 260; Bar, 20 μm.

FIGURE 3 *Amphiuma*: Region of semilysed cell at high magnification, showing one end of MB ellipse. Here, MB is characteristically multistranded and ribbonlike in appearance (arrow). Phase contrast, × 1,000; Bar, 10 μm.

preparations (21). *Amphiuma* erythrocytes in fresh blood samples are approx. 70 μm in length (Fig. 2*a*). When lysed in LyM, the centralized nuclear position of the living cell is retained. A prominent MB more than 1 μm thick is seen (Fig. 2*b–i*), generally less twisted than that of the frog. The ends of the MB appear multistranded, with the strands in a plane, ribbonlike (Fig. 3).

What holds the nucleus in place? In favorable views it can be seen that sheetlike material extends from the MB around both sides of the nucleus like a sac, suspending it in native position (Fig. 4). This trans-MB material (hereafter referred to as "TBM") gives the impression of passing around the outer edge of the MB, so that the MB is enclosed.

A third amphibian examined was the salamander, *N. viridescens*. The majority of erythrocytes in this species have eccentric nuclei (Fig. 5*a*,), and when the cells are lysed into LyM the eccentricity is retained (Fig. 5*b* and *c*). The MBs in semilysed cells of this species are also generally less twisted than those of the frog, but definitely nonplanar. Infrequently, views are obtained in which the TBM suspending the nucleus is visible (Fig. 5 *d*).

For comparative purposes, erythrocytes of the goldfish were also studied. Lysis of these cells (Fig. 6*a* and *b*) in LyM produces what at low magnification appear to be nuclei only, but careful examination under oil immersion reveals extremely thin MBs. In some preparations, the MBs do not remain attached to nuclei, but appear instead as free circles about 12 μm in diameter, or slightly less than the long axis of most of the living cells. These circles occasionally have at their periphery long, straight, tangential fibers (Fig.6*c*; see also Fig. 15*a*). In other preparations, a twisted MB is attached to the nucleus; because of its thinness, it is best visualized in uranyl-acetate-stained whole mounts in TEM (Fig. 7). Here it can be seen that the goldfish MB consists of relatively few microtubules in a tight bundle about 0.15 μm thick. A rough network of trans-MB fibrillar material (TBM) is now visible, containing fibrils of different diameters including many that

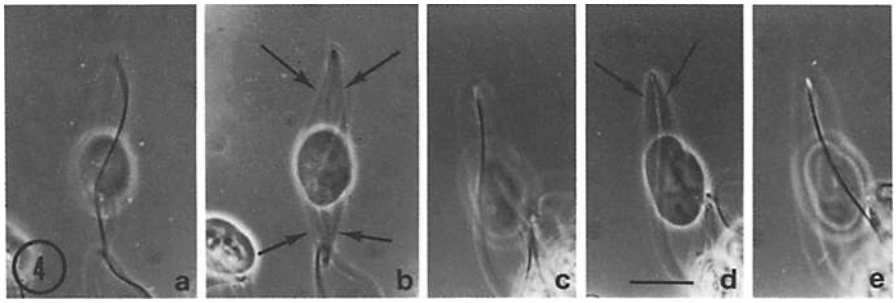


FIGURE 4 *Amphiuma*: Optical sections of two semilysed cells. Cell no. 1: (*a*) upper surface, (*b*) plane of nuclear focus. Cell no. 2: (*c*) upper, (*d*) nuclear, and (*e*) lower planes of focus. In Fig. 4*b* and *d* arrows point to material extending from MB around both sides of nucleus, apparently suspending nucleus in position. Note MB twisting in Fig. 4*a*, *c*, and *e*, and ribbonlike construction in Fig. 4*a*. Phase contrast, × 410; Bar, 20 μm.

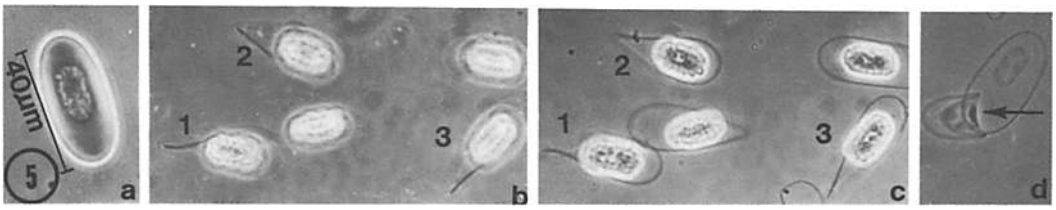


FIGURE 5 *N. viridescens*: (*a*) Living erythrocyte, with typically eccentric nucleus. (*b* and *c*) Semilysed erythrocytes, in paired views of upper (*b*) and lower (*c*) surfaces. Nuclear eccentricity is retained. (*d*) View in which TBM is visible (arrow). MBs of this species are generally less twisted in LyM than those of the frog. Phase contrast, × 410.

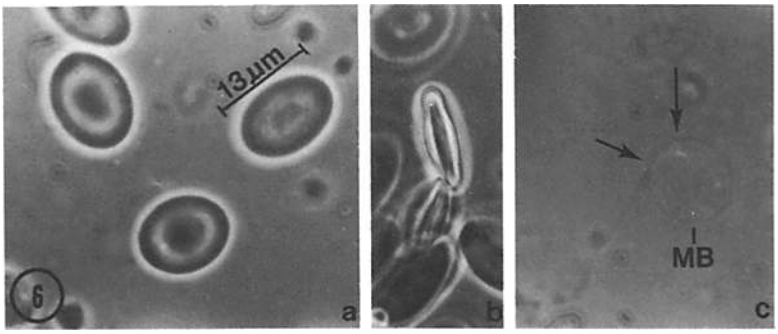


FIGURE 6 *Carassius*: (*a* and *b*) Living goldfish erythrocytes in face and edge views, respectively. (*c*) Very thin, nearly circular MB, free of nucleus in LyM (possibly difficult to see in photo reproduction). Many such free MBs have straight fibers originating at points on surface (arrows) and tangential to circle. Phase contrast, × 1,000.

are thinner than the microtubules.

Data for living and semilysed erythrocytes of the four vertebrate species are summarized in Table I.

## *Morphology of the MB in LyM*

In the species examined, the MB of semilysed cells is usually not a planar ellipse but instead assumes a twisted or bent configuration, as seen in the previous figures. The extent of twisting varies with species and even within a given preparation; it is typically most pronounced in the case of the frog, in which a majority of MBs are twisted into figure-8's.

A wire model of the typical figure-8 frog MB is shown in Fig. 8*a*. Rotation of this model about its long (Fig. 8*a–i*) and short (Fig. 8*j–p*) axis gener-

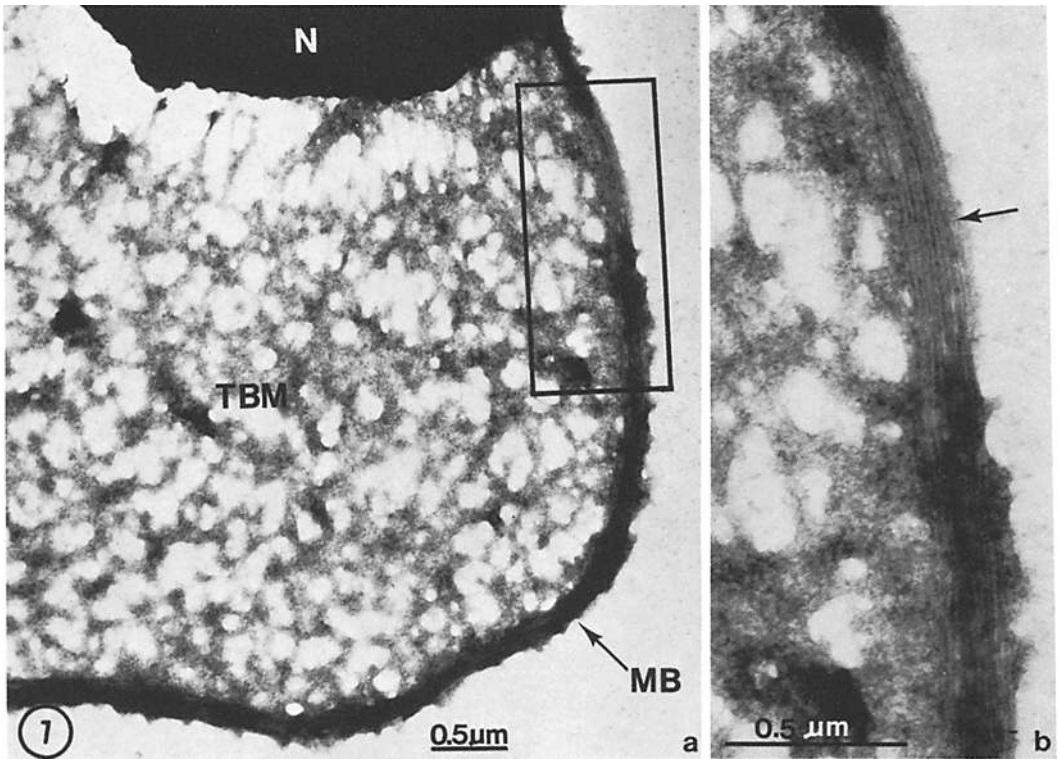


FIGURE 7 *Carassius*: (*a*) Part of a goldfish erythrocyte after lysis in LyM, as seen in uranyl acetate-stained whole mount in TEM (glutaraldehyde-fixed). Nucleus (*N*), *MB*, and network of *TBM* are visible. (*b*) Higher magnification view of rectangular area delimited in Fig. 7*a*. Where fuzzy coating of TBM is missing, 4–5 MB microtubules are visible (arrow). TEM × 19,200 and × 47,700, respectively.

TABLE I

*Summary of Morphological Characteristics for Erythrocytes and Semilysed Erythrocytes of Four Species*

| | Living Cell | | | Semilysed cell | |
|---|---|---|---|---|---|
| | Typical dimensions | | | | |
| Species | L × W | L/W | Nucleus | Nucleus | Approx. MB thickness* |
| | µm | µm | | | µm |
| *C. auratus* | 13 × 10 | 1.3 | c | c | 0.1–0.2 |
| *R. pipiens* | 25 × 17 | 1.5 | c | c | 0.2–0.3 |
| *N. viridescens* | 35 × 20 | 1.7 | e | e | 0.5 |
| *A. tridactylum* | 70 × 38 | 1.8 | c | c | >1.0 |

Abbreviations used in Table I: L, length (major axis); W, width (minor axis); c, central; and e, eccentric.

* Measured on electron micrographs of stained whole mounts for goldfish MB, and on phase-contrast micrographs along sides of MB ellipse in other species.

ates a variety of "morphological" images, many of which correspond to views of MBs in semilysed cells. Thus what initially appears to be extensive morphological variety within a semilysed preparation, such as shown in Fig. 2 for *Amphiuma*, is readily interpretable as rotated views of the same object. This is verified by studying individual figure-8 MBs as they tumble in a flow, or roll on their long axis under the cover slip (Fig. 9). The images obtained are similar to those of the wire model (Fig. 8*c–h*), and more mildly twisted versions of the same model account for most views of

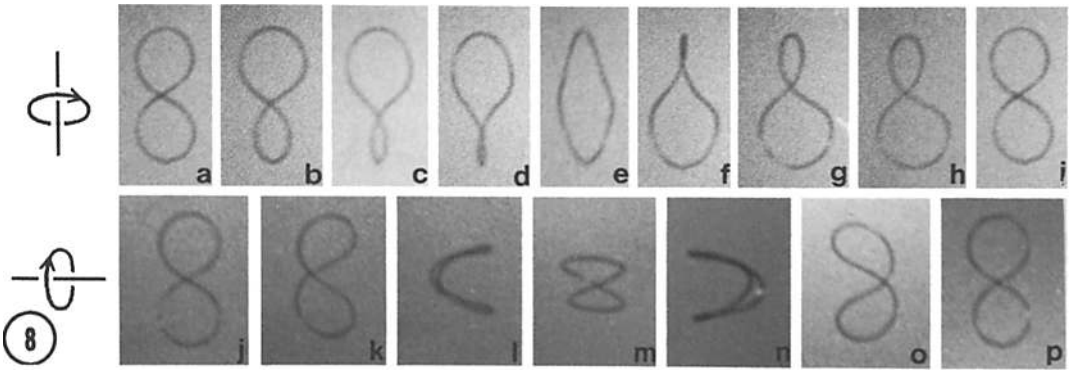


FIGURE 8 A three-dimensional wire model of the "figure-8" frog MB, rotated about its long axis (*a–i*) and about its short axis (*j–p*). The views obtained can account for many of the "variations" of MB morphology observed in semilysed cell preparations (note, for example, correspondence to *Amphiuma* MBs in Fig. 2).

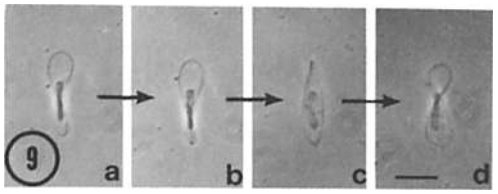


FIGURE 9 *N. viridescens*: Sequential views of one MB as it rolls on its long axis under the cover slip. (*a*) Upper loop larger than lower, (*b*) lower loop smaller than in Fig. 9*a*, (*c*) both loops gone, (*d*) lower loop slightly larger than upper loop. These views correspond to some of those in Fig. 8*c–h*. Phase contrast, × 260; Bar, 20 μm.

more mildly twisted MBs in *Amphiuma* and *Notophthalmus* preparations.

An interesting feature of the model is that it has a physically distinct mirror image (Fig. 10). Thus, the two mirror-image models (I, right-handed twist; II, left-handed twist) are not interconvertible by rotation or inversion. The question therefore arises as to whether a given species or preparation presents both mirror images in roughly equal numbers, or whether there exists nonrandomness or preferential twisting. This problem was studied in frogs (*R. pipiens* and *R. catesbiana*) and salamanders (*N. viridescens*) by unidirectional fine-focusing through large numbers of MBs to determine upper surface MB cross-over direction in the figure-8 view or location of high and low points in the 90° rotated view (Fig. 10). 50 MBs in non-overlapping fields were tabulated according to model type in five preparations per species, each from a different animal. The results (Table II) show that twist direction is nonrandom in each species, heavily favoring model I (right-handed). In the two frog species model II MBs rarely occur, while in *N. viridescens* only about 20% are model II. A mirror-image pair (*N. viridescens*) is shown in Fig. 11, with model I on the left, model II on the right. In Fig. 5*b* and *c* (*N. viridescens*), a somewhat different view, MB no. 1 is model II while MBs nos. 2 and 3 are model I. The two *R. pipiens* MBs in Fig. 1 are also seen to be model I. Although not studied by detailed counts, model I MBs appear predominant in *Amphiuma* as well (e.g., all those in Fig. 2).

As tested with *R. pipiens*, twist direction is unrelated to animal storage temperature; model I MBs typify preparations from both cold-stored and room temperature-acclimated frogs (Table II, animals 1–4 vs. 5). Nonrandom twisting is not attributable to normal preparative mechanical forces either, since model I MBs also characterize semilysed cells prepared by on-slide perfusion of whole blood with LyM.

## *Morphology of the MB in situ*

In order to assess the initial extent of MB twisting *in situ*, on-slide perfusion experiments were performed. Erythrocytes were photographed as a moving "front" of LyM passed over them, thereby showing individual cells just before and just after semilysis. As seen in Fig. 12, *Amphiuma* MBs are not twisted noticeably at the moment of lysis; the MBs are apparently much more planar *in situ* than they later appear in the LyM preparations. In addition, it is clear that the spread or flattened ends of the MB ellipse correspond to the ends of the cell *in situ*. Similar perfusion experiments with erythrocytes of *R. pipiens* demon-

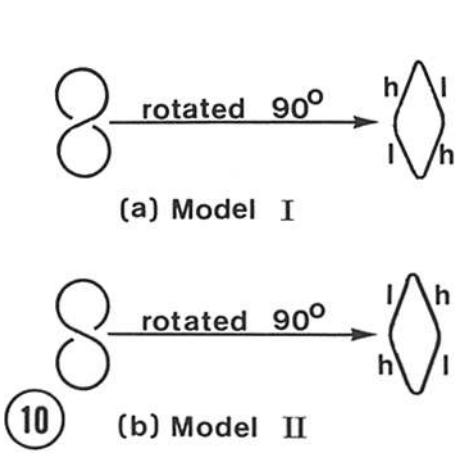


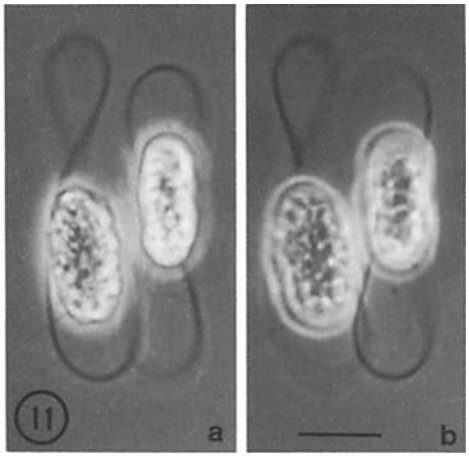


FIGURE 10 Diagram of the possible mirror-image models of figure-8 MBs. (*a*) Model I, right-handed twist with cross-over from lower left to upper right; when rotated 90° in either direction, its surface high points (*h*) are at lower right and upper left. Low points (*l*) at lower left and upper right. (*b*) Model II, left-handed twist with cross-over from lower right to upper left; with 90° rotation, high points are at lower left and upper right.

FIGURE 11 *N. viridescens*: A pair of semilysed cells in which the MBs exhibit mirror-image twisting. (*a*) Focus on upper surfaces of each, and (*b*) lower surfaces. The MB to the left corresponds to model I of Fig. 10; MB on right corresponds to model II. Phase contrast, × 1,050; Bar, 10 μm.

TABLE II

*MB Twist Direction in Semilysed Erythrocytes of Different Species*

| | No. of model I MBs/no. of model II MBs‡ | | | | | | |
|---|---|---|---|---|---|---|---|
| | Animal | | | | | | |
| Species* | 1 | 2 | 3 | 4 | 5 | Total | Model I |
| | | | | | | | % |
| *R. pipiens* | 50/0 | 50/0 | 50/0 | 50/0 | 49/1 | 249/1 | 99.6 |
| *R. catesbiana* | 50/0 | 50/0 | 50/0 | 49/1 | 50/0 | 249/1 | 99.6 |
| *N. viridescens* | 42/8 | 35/15 | 42/8 | 41/9 | 42/8 | 202/48 | 80.8 |

* *R. pipiens* animal no. 5 and all *N. viridescens* were acclimated to room temperature; other animals were cold-stored (see Materials and Methods). Cells of *R. catesbiana* were washed in amphibian Ringer's solution (15) before use.

‡ Tabulation for 50 MB's in each preparation, one preparation per animal.

strated that MBs of these cells were also relatively planar *in situ*.

## *Release of Free MBs from Semilysed Cells*

LyM preparations (*R. pipiens, Amphiuma*), when left at room temperature for 18–48 h, sometimes developed bacterial growth which selectively digested nuclei and, apparently, most of the TBM. As seen in Fig. 13, resulting free *Amphiuma* MBs are generally untwisted, retaining ellipticity and the ribbonlike differentiation into multiple strands at their ends (Fig. 3). The latter was evident even in transsected MBs which had opened to a more linear configuration (Fig. 13*c*).

Negative staining of such free MBs (*Amphiuma*) for TEM reveals the individual microtubules. The major bundle comprising the MB is generally too thick and dense for observation, but twisted ribbonlike groups of a few microtubules often "fray" out so as to provide clear views of their closely adjacent surfaces (Fig. 14). Similar

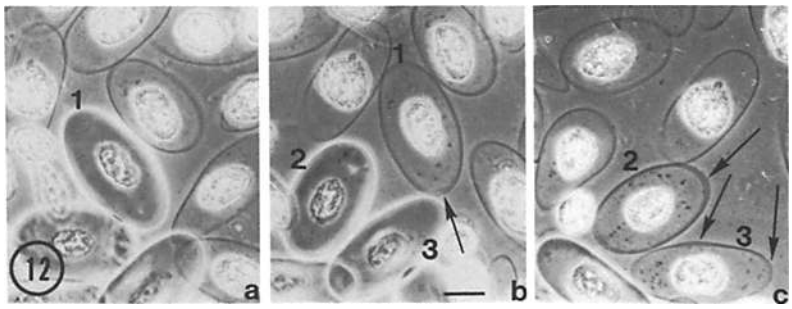


FIGURE 12 *Amphiuma*: Erythrocytes just before and after exposure to LyM by perfusion. Cell no. 1 (*a*) is shown again in semilysed state (*b*) just after loss of hemoglobin. Similarly, cells nos. 2 and 3 (*b*) are shown again semilysed in Fig. 12*c*. Note ribbonlike appearance at ends and side of MB ellipse, seen immediately upon lysis (*b* and *c*; arrows). Little MB twisting is initially evident. Phase contrast, × 260; Bar, 20 μm.

but more extensive sheetlike microtubule arrays are also evident in thin internal areas or at MB edges.

Slow release of free MBs by apparent long-term bacterial digestion suggested that rapid release might be achieved through use of high concentrations of digestive enzymes. Trypsin and pepsin were tested in LyM (TAME omitted), and both enzymes produced free MBs. At final cell concentrations of approx. $10^6$ cells/ml, trypsin was useful at 0.01 mg/ml. A majority of MBs were released in minutes, with nuclei gradually getting smaller and disappearing in about 10 min. At higher trypsin concentrations MBs were also released, but nuclei lysed rapidly, forming a gel in which MBs were trapped. Pepsin was ineffective at similar concentrations (no doubt due in part to the far-from-optimal pH for pepsin activity), but at very high concentrations (20 and 10 mg/ml) a majority of MBs and nuclei were liberated intact within minutes, and nuclei did not dissolve (Figs. 15 and 16). At lower pepsin concentrations (1, 2.5, and 5 mg/ml), the same result was obtained but it took progressively longer. MB release occured with pepsin present either initially or added just after lysis.

MBs freed by proteolysis exhibit little of the three-dimensional twisting evident in semilysed cells. However, their most striking feature is their relative circularity when compared with living cells (Figs. 15 and 16). Pepsin-released MBs of *R. pipiens* and *N. viridescens* have length-to-width (L/W) ratios of about 1.09 and 1.04, respectively (average for 10 MBs each), vs. about 1.44 and 1.73 for living cells of the two species (average for 10 cells each). Similarly, the free *Amphiuma* and goldfish MBs (as in Figs. 13 and 6) have average L/W ratios of 1.34 and 1.08 (for 10 MBs each) vs. 1.81 and 1.38, respectively, for living erythrocytes (average of 10 cells each). It was evident, therefore, that they must undergo a process of circularization concomitant with MB and nuclear release. This "ellipse-to-circle" transformation was followed in time-course photographs of individual semilysed cells incubating in media containing pepsin (Fig. 16).

With incubation of free MBs in pepsin over longer periods, many showed evidence of partial breakdown. The most common occurrences were transsected *R. pipiens* MBs which were initially S-shaped, and MBs of *N. viridescens* with tangential straight segments which appear to have peeled away from part of the circle (Fig. 15*a*). The latter are similar to those of the goldfish (Fig. 6*c*), except that the segments are thicker or multiple. Also common in *N. viridescens* preparations were more advanced stages of disorganization in which there remain only short MB arcs with straight fibers frayed out at both ends (Fig. 15*b*). For initial location and observation of free MBs at low magnification, the darkfield effect (Fig. 15*c*) proved more useful than phase contrast. Free MBs were also found to be birefringent (Fig. 15*d*), exhibiting alternating 90° arcs of bright and dark contrast in polarized light.

Free MBs showed evidence of considerable structural stability; they were impaled on microneedles and shaken side-to-side without apparent damage (Fig. 17). If transsected by pressure of the microneedle against the slide, they opened outward immediately into a more linear configuration.

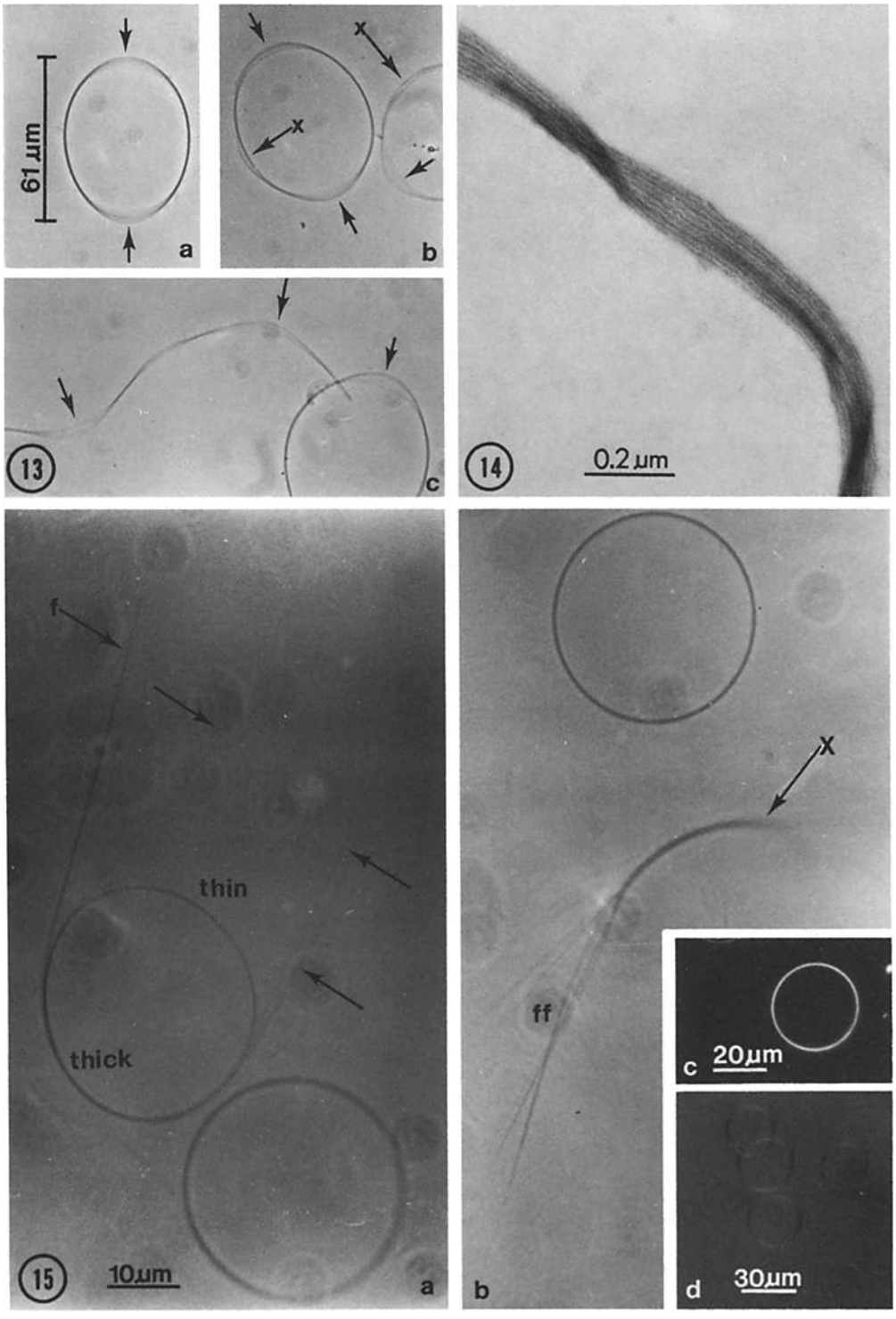
61 µm
a
x
x
b
13
c
14
0.2 µm
f
thin
thick
15
10µm
a
x
ff
b
c
20µm
d
30µm

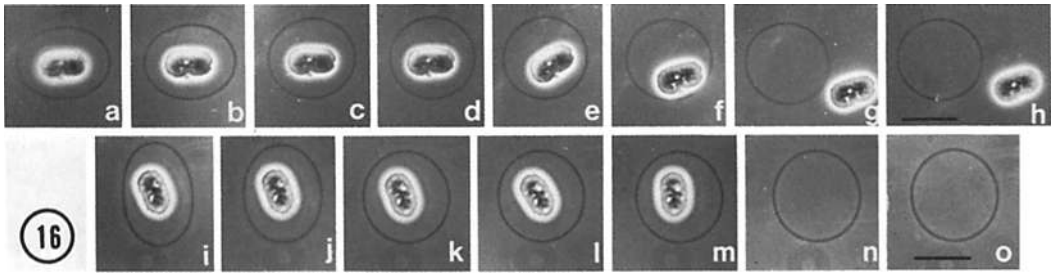


FIGURE 16 *N. viridescens*: "Ellipse-to-circle" transformation of MBs during release from semilysed cells by pepsin digestion. Cells added to LyM (TAME omitted) containing pepsin at t = 0. (*a–h*) Time-course, pepsin 20 mg/ml: (*a*) t = approx. 45 s, MB still elliptical, nucleus in place; (*b* and *c*) 15-s intervals; (*d*) t = 90 s, MB nearly circular, nucleus still in position; and (*e*) t = 105 s, nucleus and MB begin to drift apart; (*g* and *h*), at t = 5 min, tapping on cover slip shows that nucleus and MB are completely free of each other. Sequence (*i–o*): time-course at lower pepsin concentration (5 mg/ml), in 5-min intervals beginning at (*i*) t = 10 min, with MB elliptical and nucleus in position; (*k*) t = 20 min, MB nearly circular; (*l*) t = 25 min, nucleus drifting; and (*n* and *o*) nucleus gone after tapping on cover slip. Bars, 20 μm. Phase contrast, × 365.

## DISCUSSION

### *Morphological and Mechanical Properties of Nucleated Erythrocytes: A Working Hypothesis*

The results indicate that MBs are discrete bundles of microtubules bound together so as to form mechanically functional units. When freed from semilysed cells, MBs of the various species observed here tend to circularize, and this is also the case for MBs of *Triturus cristatus* isolated by a nonproteolytic method (8). For the MB alone, circularity therefore appears to be the preferred state, with external forces required for *in situ* maintenance in an elliptical form. As a working hypothesis, it is proposed that the TBM is normally under tension, applying such forces asymmetrically across the MB. The otherwise more circular MB (and the cell) would thus be converted to an ellipse, with TBM tension accounting for cell flatness as well. Both MB and TBM acting together as a system would be required to produce the flattened elliptical morphology of nucleated erythrocytes.

According to this hypothesis, protease digestion

FIGURE 13 *Amphiuma*: Free MBs, prepared by storage of a fresh LyM preparation for 18 h at room temperature. Nuclei and TBM have apparently been digested by bacteria which are observed growing in the preparation. Most free MBs retain ellipticity (*a*) and their characteristically ribbonlike ends (*a–c*, plain arrows; cf. Figs. 3 and 12). A few free MBs are broken, and are opened outward into a more linear state in which the original differentiated ribbonlike ends are still readily apparent (*c*, arrows). In some intact free MBs the normally compact sides also appear multistranded, as if the view there might be that of a ribbon presented edge-on (*b*, arrows labeled *X*). Phase contrast, × 410.

FIGURE 14 *Amphiuma*: Uranyl acetate-stained strand "frayed" out of the major MB bundle; free MBs prepared as described in Fig. 13. Strand consists of four closely applied microtubules in a twisted (not braided) sheet. Lumen of each microtubule has taken up stain. TEM, × 68,300.

FIGURE 15 *N. viridescens*: Free MBs released from semilysed cells by pepsin digestion in LyM lacking TAME. The MBs appear to be planar and almost circular. (*a* and *b*) Examples of both intact MBs and MBs in states of disorganization after 2 h exposure to pepsin. (*a*) Long, thin, straight fibers (arrows) originating at surface of one MB, and tangential to it at points of origin. Note similarity to the *Carassius* preparation in Fig. 6*c*. The relatively thick fiber (arrow *f*) as well as others have evidently peeled away from one side of the MB, leaving it thinner than opposite side. (*b*) One MB intact, one highly disorganized. Multiple fibers (*ff*) are frayed out at one end of a short MB arc; similar fibers are present at other end (*X*) but are out of plane of focus. (*a* and *b*) Phase contrast, × 1,050. (*c*) Intact, free MB in darkfield, × 410. (*d*) Birefringence of free MBs, with background light intensity adjusted to show alternating arcs of bright and dark contrast. Polarization microscopy, × 265. Pepsin 20 mg/ml in all cases.

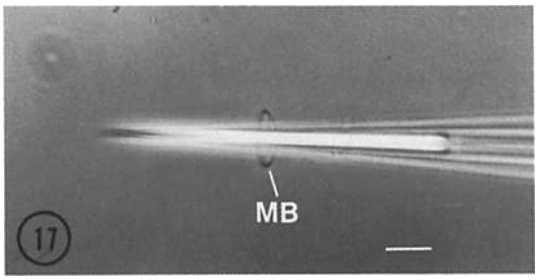


FIGURE 17 *C. pyrroghaster*: Micromanipulation of trypsin-freed MB; equal volume of LyM added to preparation after MB release, to slow proteolysis. The microneedle was freely movable within the MB circle, indicating absence of TBM. In this and other experiments, MBs remained intact during side-to-side shaking and general micromanipulation while on needles. Bar, 20 $\mu$m. Phase contrast, × 300.

of the TBM releases the asymmetric tension, permitting the MB to circularize without change in circumference. The latter point is verified by direct measurement of MB circumference or by its calculation from axial dimensions (44) during the "ellipse-to-circle" transformation (Fig. 16). Circularization of free MBs is suggestive of uniform redistribution of internal strain, with the strain inherent due to bending of straight structural components. Release of such strain provides a simple explanation for the straightness of fibers which peel free in disorganizing MBs (Figs. 6*c* and 15*a*), and for the increased linearity and opening outward of MBs transsected either microsurgically or accidentally during preparation (Fig. 13*c*).

The figure-8 MB configuration lends support to the idea that the TBM can sustain a tension, and that it has elastic or contractile properties which can deform the MB. The figure-8 MB corresponds to the edge, or frame, of a hyperbolic paraboloid surface (39). This is a curved, saddle-shaped surface of reduced area, produced by networks or sheets of material under tension, as in "warped" tennis rackets or frames with overstretched canvas. Such a surface is readily reproduced by soap films on figure-8 wire models. Since figure-8 MBs are prevalent only when TBM is present, they are directly interpretable as the result of extreme TBM shrinkage or contraction. Curvature of the TBM is, in fact, visible in some fortuitous views of semilysed cells (e.g., Fig. 5*d*, arrow). MB deformation is then seen as an accommodation to reduction in TBM surface area compared with that present in normal living cells and initially (Fig. 12) in semilysed cells.

The proposed combination of MB strain and TBM tension results in a system with flexibility and deformability, as well as the potential for returning rapidly to normal equilibrium morphology upon removal of deforming forces. These are desirable properties with respect to erythrocyte function. In addition, TBM pressure against nuclei would account for their positional stability (Table I) and for the nuclear bulge seen in all such cells viewed edgewise (e.g., Fig. 6*b*). Conversely, the metabolically inactive nuclei (25, 27) might be retained as structurally stabilizing "hubs."

### *Properties of the TBM*

The TBM of the semilysed erythrocyte is nearly transparent in phase contrast, and is not readily visible by this means except in tangential views of the larger cell species (Fig. 4). It is apparently responsible for interconnecting nucleus and MB, and for holding the nucleus in native position (eccentric in *N. viridescens*, central in the others). In TEM whole mounts, the TBM appears as a rough network spanning the space between nucleus and MB, and attached to or wrapped around the latter. In some regions, fine fibrillar material is present. Since the TBM passes around opposite sides of the nucleus (Fig. 4), the image obtained in TEM whole mounts is presumably complicated by the presence of two networks collapsed onto each other.

The action of proteases on semilysed cells implicates protein as a constituent of the TBM or its connections to nucleus and MB. Microfilament proteins and associated species such as spectrin are likely structural candidates. A spectrin-actin network is thought to exist in human erythrocyte ghosts (41), in which actin, myosin, and spectrin are retained after treatment with concentrations of Triton X-100 similar to that employed in this work (38). Mammalian blood platelets, which contain MBs (5, 36), have long been known to contain in addition the contractile actomyosin-like complex thrombosthenin (11), which is probably associated with platelet shape changes (7, 23, 47). It should be noted, however, that the hypothesis presented above does not *require* the TBM to be actively contractile.

Has material corresponding to the TBM of semilysed nucleated erythrocytes been observed previously? A number of early light microscopists described stained peripheral networks within mature amphibian erythrocytes (2, 18, 19, 30, 33, 43), some of which were dismissed as artifacts. More re-

cently Shinagawa (37) demonstrated a"reticulum" in silver-stained mature erythrocytes of diverse vertebrate species, tentatively identifying it as endoplasmic reticulum, but suggesting a fibrous protein composition due to insolubility in fat solvents. It is likely that in at least some of these cases the equivalent of TBM has been observed.

### *MB Morphology*

MBs, especially the thicker ones of large erythrocytes, appear ribbonlike (rather than cylindrical) in construction. This is particularly clear at the ends of the MB ellipse both in semilysed cells and in free MBs (Figs. 3, 12, and 13), but can also be detected along the sides of MBs (Figs. 12 and 13). In addition, ribbonlike shape was shown for free MBs of *T. cristatus* by Bertolini and Monaco (8), and the description is applicable to MB microtubule arrangements observed in thin sections through erythrocytes of various species (4, 5, 21).

There is a general positive correlation between erythrocyte size and MB thickness (Table I); presumably this reflects the number of microtubules per MB cross section and is of mechanical significance. The *Amphiuma* MB contains hundreds of microtubules, vs. about eight for the goldfish (45) and about 25 for the frog (6). Direct measurement of MB thickness in semilysed cells therefore supports the correlation between cell size and MB microtubule number adduced by Goniakowska-Witalińska and Witaliński (24) for vertebrates in general. Since free MBs are birefringent (Fig. 15*d*), quantitative measurements of the coefficient of birefringence might be useful in estimating microtubule number (22) or in testing such a correlation in this system.

Although extensive figure-8 MB twisting apparently does not occur normally in vivo, the phenomenon is potentially informative, as indicated in the discussion above. Nonrandomness of twist direction shows repeatability with different animals of each species tested (Table II), and is probably symptomatic of some regular feature of TBM/MB construction. Among several possibilities are the nonrandom distribution of MB/TBM attachment points, and asymmetry in the pattern of intra- or inter-microtubule bonding. Should the latter result in some degree of directional internal MB twisting (as in a Möbius strip [48] with a 180° clockwise vs. counterclockwise twist, for example), this would further bias the figure-8 MB twist direction.

There have been occasional previous observations of figure-8 MB twisting *in situ*. Such configurations are among several variations illustrated by Meves (33) for stained amphibian erythrocytes, and loops or figure-8's were also reported by Fawcett and Witebsky (21) and Behnke (6) in *Amphiuma* and in cold-treated frog erythrocytes, respectively. Twisting of intact, unstained cells (observed as well in the present work on occasion), attributable to MB twisting in vivo, has also been described (6, 33).

### *The Semilysed Erythrocyte Model System*

Lysis of nucleated erythrocytes in LyM provides an experimentally accessible cell model system which should be useful for further analysis of MB/TBM properties. This system is analogous to "semilysed" mitotic cells studied by others (14, 32) and to cell models in general (28) in being freely permeable and readily subject to experimental conditions. A similar approach may be fruitful in examining or revealing MBs in other cell types, including "blood" cells of certain invertebrates (16), nonmammalian vertebrate thrombocytes (21), mammalian platelets (5, 36), mammalian erythrocytes of the camel family (3), and fetal nucleated erythroblasts of at least one mammalian species, the rabbit (26). MBs have apparently not been identified as such in human erythroblasts, but it is possible that "Cabot rings" (9, 10, 13) are MBs. These threadlike closed circles and figure-8's (13, 31) have staining characteristics similar to those of mitotic spindle remnants (which contain microtubules), and are a clinical manifestation of severe human anemias in which nucleated erythrocytes are present in the blood (10, 12, 13, 34, 40, 42).

For their interest, assistance, and helpful discussion, I am indebted to my students and colleagues, especially Drs. M. Cohen, E. S. Handler, and E. Shahn. I wish also to thank Dr. L. B. Cohen for kindly lending the micromanipulator, and Dr. R. G. Zweiful for assisting in species identification.

This work was supported by City University of New York PSC/BHE grant no. 11619, and by National Institutes of Health grant no. HL20902 from the National Heart, Lung, and Blood Institute.

*Received for publication 12 May 1977, and in revised form 23 February 1978.*

## REFERENCES

1. ANDREW, W. 1965. Comparative Hematology. Grune & Stratton, Inc. New York.
2. AVEL, M. 1924. Sur l'appareil de golgi des hématies

de Grenouille. *C. R. Soc. Biol.* **90:**792–794.
3. BARCLAY, N. E. 1966. Marginal bands in duck and camel erythrocytes. *Anat. Rec.* **154:**313.
4. BARRETT, L. A., and R. B. DAWSON. 1974. Avian erythrocyte development: microtubules and the formation of the disk shape. *Dev. Biol.* **36:**72–81.
5. BEHNKE, O. 1965. Further studies on microtubules. A marginal bundle in human and rat thrombocytes. *J. Ultrastruct. Res.* **13:**469–477.
6. BEHNKE, O. 1970. A comparative study of microtubules of disk-shaped blood cells. *J. Ultrastruct. Res.* 31:61–75.
7. BEHNKE, O., B. I. KRISTENSEN, and L. E. NIELSEN. 1971. Electron microscopical observations on actinoid and myosinoid filaments in blood platelets. *J. Ultrastruct. Res.* **37:**351–369.
8. BERTOLINI, B., and G. MONACO. 1976. The microtubule marginal band of the newt erythrocyte. *J. Ultrastruct. Res.* **54:**59–67.
9. BESSIS, M. 1956. Cytology of the Blood and Blood-Forming Organs. Grune & Stratton, Inc. New York.
10. BESSIS, M. 1973. Living Blood Cells and their Ultrastructure. Springer-Verlag New York, Inc., New York.
11. BETTEX-GALLAND, M. and E. F. LÜSCHER. 1959. Extraction of an actomyosin-like protein from human thrombocytes. *Nature (Lond.).* **184:**276–277.
12. BOSTRÖM, L. 1947. La formation des anneaux de Cabot. Sang. **18:**67–68.
13. CABOT, R. C. 1903. Ring bodies (nuclear remnants?) in anemic blood. *J. Med. Res.* **9** (*New Ser., 4*)**:**15–18.
14. CANDE, W. Z., J. SNYDER, D. SMITH, K. SUMMERS, and J. R. MCINTOSH. 1974. A functional mitotic spindle prepared from mammalian cells in culture. *Proc. Natl. Acad. Sci. U. S. A.* **71:**1559–1563.
15. CAVANAUGH, G. M., editor. 1975. Formulae and Methods VI of the Marine Biological Laboratory Chemical Room. The Marine Biological Laboratory, Woods Hole, Mass. 6th edition.
16. COHEN, W. D., I. NEMHAUSER, and R. JAEGER. 1977. Rapid visualization of the marginal band system in blood cells of marine species. *Biol. Bull, (Woods Hole).* **153:**420.
17. CONANT, R. 1958. A Field Guide to Reptiles and Amphibians. Houghton Mifflin Company, Boston, Mass.
18. DAWSON, A. B. 1929. A further study of the reaction of the amphibian erythrocyte to vital dyes, osmic acid, and silver salts, with special reference to basophilia and reticulation. *Anat. Rec.* **42:**281–300.
19. DEROO, G. I., and E. H. UFFORD 1930. An investigation of the staining reactions of erythrocytes of the leopard frog to nile-blue sulphate, with special reference to the nature of the segregation apparatus and the Golgi substance. *Anat. Rec.* **46:**297–304.
20. FAWCETT, D. W. 1959. Electron microscopic observations on the marginal band of nucleated erythrocytes. *Anat. Rec.* **133:**379.
21. FAWCETT, D. W., and F. WITEBSKY. 1964. Observations on the ultrastructure of nucleated erythrocytes and thrombocytes with particular reference to the structural basis of their discoidal shape. *Z. Zellforsch.* **62:**785–806.
22. FORER, A. 1976. Actin filaments and birefringent spindle fibers during chromosome movements. *In* Cell Motility. R. Goldman, and T. Pollard, editors. Cold Spring Harbor Laboratory, Cold Spring Harbor, N. Y. 1273–1293.
23. GERRARD, J. M J. G. WHITE, and G. H. R. RAO. 1974. Effects of the ionophore A23187 on blood platelets. II. Influence on ultrastructure. Am. J. Pathol. **77:**151–166.
24. GONIAKOWSKA-WITALIŃSKA, L., and W. WITALIŃSKI. 1976. Evidence for a correlation between the number of marginal band microtubules and the size of vertebrate erythrocytes. *J. Cell Sci.* **22:**397–401.
25. GOTO, S., and N. R. RINGERTZ. 1974. Preparation and characterization of chick erythrocyte nuclei from heterokaryons. *Exp. Cell Res.* **85:**173–181.
26. GRASSO, J. A. 1966. Cytoplasmic microtubules in mammalian erythropoietic cells. *Anat. Rec.* **156:**397–414.
27. HARRIS, H. 1965. Behavior of differentiated nuclei in heterokaryons of animal cells from different species. *Nature (Lond.).* **206:**583–588.
28. HOFFMAN-BERLING, H. (1960). Other mechanisms producing movements. *In* Comparative Biochemistry II, Academic Press, Inc., New York. 341–369.
29. INOUÉ, S., G. G. BORISY and D. P. KIEHART. 1974. Growth and lability of *Chaetopterus* oocyte mitotic spindles isolated in the presence of porcine brain tubulin. *J. Cell Biol.* **62:**175–184.
30. JORDAN, H. E. 1925. A study of the blood of the leopard frog, by the method of supravital staining combined with the injection of India ink into the dorsal lymph sac, with special reference to the genetic relationships among leucocytes. *Am. J. Anat.* **35:**105–132.
31. JORDAN, H. E., J. E. KINDRED, and H. W. BEAMS. 1930. The relation of Cabot rings to the reticulofibrillar apparatus of Golgi. *Anat. Rec.* **46:**139–160.
32. MCGILL, M., and B. R. BRINKLEY. 1975. Human chromosomes and centrioles as nucleating sites for the *in vitro* assembly of microtubules from bovine brain tubulin. *J. Cell Biol.* **67:**189–199.
33. MEVES, F. 1911. Gesammelte Studien an den roten Blutkörperchen der Amphibien. *Archiv. Mikroskop. Anat.* **77:**465–540.
34. PICARD, D. 1953. Nature et signification des anneaux de Cabot des hématies. *CR Soc. Biol.* **1472:**1451–1453.
35. REBHUN, L. I., J. ROSENBAUM, P. LEFEBRE, and G. SMITH. 1974. Reversible restoration of the birefringence of cold-treated, isolated mitotic appa-

ratus of surf clam eggs with chick brain tubulin. *Nature (Lond.)*. **249**:113–115.

36. SANDBORN, E. B., J. LEBUIS, and P. BOIS. 1966. Cytoplasmic microtubules in blood platelets. *Blood*. **27**:247–252.
37. SHINAGAWA, C. 1960. Morphological and cytochemical studies on erythrocytes of vertebrates. *J. Sci. Hiroshima Univ., Ser. B. Div. 1: Zool.* **19**:57–116.
38. STECK, T. L. 1974. The organization of proteins in the human red blood cell membrane. *J. Cell Biol.* **62**:1–19.
39. STEINHAUS, H. 1960. Mathematical Snapshots. Oxford University Press, New York.
40. TANAKA, Y., and J. R. GOODMAN. 1972. Electron Microscopy of Human Blood Cells. Harper, Row Publishers, Inc., New York.
41. TILNEY, L. G., and P. DETMERS. 1975. Actin in erythrocyte ghosts and its association with spectrin. *J. Cell Biol.* **66**:508–520.
42. VAN OYE, E. 1954. L'origine des anneaux de Cabot. *Rev. Hematol.* **9**:173–179.
43. VON SMIRNOW, A. E. 1906. Die prolongierte Osmiummethode nach Fr. Kopsch als ein Mittel zur Darstellung einiger Strukturen in den Erythrocyten des Siredon pisciformis. *Anat. Anz.* **29**:236–241.
44. WEAST, R. C., and S. M. SELBY, editors. 1967. CRC Handbook of Tables for Mathematics. The Chemical Rubber Co., Cleveland, Ohio. 3rd edition. p. 12.
45. WEINREB, E. L., and WEINREB, S. 1965. Studies on the fine structure of teleost blood cells. II. Microtubular elements of erythrocyte marginal band. *Z. Zellforsch. Mikrosk. Anat.* **68**:830–836.
46. WEISENBERG, R. C. 1972. Microtubule formation *in vitro* in solutions containing low calcium concentrations. *Science (Wash., D. C.)*. **177**:1104–1105.
47. WHITE, J. G., G. H. R. RAO, and I. M. GERRARD. 1974. Effects of the ionophore A23187 on blood platelets. I. Influence on aggregation and secretion. *Am. J. Pathol.* **77**:135–150.
48. WILLARD, S. 1970. General Topology. Addison-Wesley Publishing Co., Reading, Mass. p. 63.